IEEE Access
Multidisciplinary | Rapid Review | Open Access Journal

SPECIAL SECTION ON WIRELESS CACHIING TECHNIQUE FOR 5G

Received November 11, 2016, accepted December 6, 2016, date of publication December 13, 2016, date of current version March 13, 2017.

Digital Object Identifier 10.1109/ACCESS.2016.2639035

A Small-Cell Caching System in Mobile Cellular Networks With LoS and NLoS Channels

JUN LI[1], (Senior Member, IEEE), YOUJIA CHEN[2], MING DING[3], (Member, IEEE), FENG SHU[1], (Member, IEEE), BRANKA VUCETIC[2], (Fellow, IEEE), AND XIAOHU YOU[4], (Fellow, IEEE)

[1]School of Electronic and Optical Engineering, Nanjing University of Science and Technology, Nanjing 210094, China
[2]School of Electrical and Information Engineering, The University of Sydney, Sydney, NSW 2006, Australia
[3]Data61, Commonwealth Scientific and Industrial Research Organization Australia, Sydney, NSW 2015, Australia
[4]National Mobile Communications Research Laboratory, Southeast University, Nanjing 210096, China

Corresponding author: Y. Chen (youjia.chen@sydney.edu.au)

ABSTRACT Small-cell caching utilizes the embedded storage of small-cell base stations (SBS) to cache popular network contents, for the purpose of reducing duplicate transmissions in mobile networks and offloading the data traffic from macro-cell base stations. In this paper, we propose a random small-cell caching system, where each SBS randomly caches a subset of popular contents with a specified caching probability. We particularly focus on the probability that mobile users can successfully download their requested files from the SBSs, namely, successfully downloading probability (SDP). A sophisticated path-loss model incorporating both line-of-sight (LoS) and non-LoS (NLoS) transmissions is introduced into the SDP analysis. By modeling the distribution of the SBSs as a Poisson point process, we develop theoretical results of the SDP performance based on stochastic geometry theory. Additionally, we investigate the impacts of the parameters of the SBSs, i.e., transmission power and deployment intensity, on the SDP. Monte Carlo simulations show the consistency with our derived SDP. Also, numerical results validate our analysis on the related parameters and their impacts on the SDP performance.

INDEX TERMS Wireless caching, content-centric communications, small-cell networks, stochastic geometry, NLoS channels.

I. INTRODUCTION

Wireless data traffic has been increasing dramatically in recent years due to the proliferation of smart mobile devices and various mobile applications. The driving forces behind this traffic growth have fundamentally shifted from being the steady increase in demand for connection-centric communications, such as phone calls and text messages, to the explosion of content-centric communications, such as mobile video streaming and content sharing. Network traffic observation indicates that mobile users' requests usually concentrate on a small portion of popular contents, e.g., movies and blockbusters [1], thereby leading to a large amount of duplicate transmissions of these contents. Motivated by this observation, intelligently caching some popular contents into network nodes has been proposed to effectively reduce the duplicate transmissions as well as offload data traffic from macro-cell base stations [2]. Caching in 3G and 4G mobile networks is shown to be able to reduce the traffic by one third to two thirds [3]–[5].

Generally, wireless caching consists of two phases: a content placement phase and a content delivery phase [6]. In the content placement phase, popular contents are cached into the storage units of network nodes that are close to mobile users (MU). In the content delivery phase, the cached popular contents can be quickly retrieved to serve the MUs. Usually, the content placement phase is carried out during off-peak hours. In this sense, caching can shift the traffic load from peak hours to off-peak hours, alleviating the backhaul congestion.

Several caching strategies for wireless networks have been proposed recently. The authors in [7] analyzed the strategy of caching contents in the Evolved Packet Core of the LTE networks. In [8] and [9], the authors studied the strategy of caching in radio access networks, with an aim to push the contents even closer to the MUs. The concept of "Femtocaching" proposed in [9] and [10] utilized femtocell base stations in heterogeneous cellular networks as distributed caching devices. Additionally, caching strategies

for the device-to-device (D2D) networks were investigated in [11]–[13], where each mobile terminal caches part of popular contents and exchanges information with each other via D2D communications.

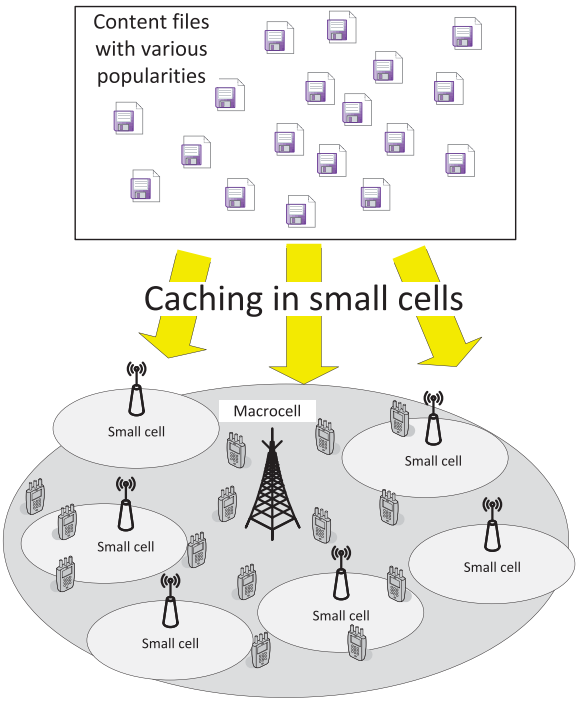

FIGURE 1. The system model of small-cell caching.

Since currently small-cell base stations (SBS) have been widely deployed in heterogeneous cellular networks [14], this dense deployment of SBSs provides a basis for implementing the caching technology, referred to as small-cell caching, as illustrated in Fig. 1. In the small-cell caching, popular contents are cached into the storage of SBSs, and ready to be fetched by the MUs. Current research on the small-cell caching mainly focuses on the deterministic placement, where contents are placed and optimized for fixed networks, i.e., assuming that the locations of network nodes and the channel state information are known beforehand [9], [15]. However, in practice, the distribution of the SBSs and the wireless channels vary from time to time.

In this paper, we consider a random small-cell caching system, in which each SBS randomly caches a subset of popular contents with a specified caching probability. We consider such a system in the context of a stochastic network, where the distribution of SBSs follows a Poisson point process, the wireless channels in the network are Rayleigh fading, and the path-loss model embraces both line-of-sight (LoS) and non-line-of-sight (NLoS) paths. To evaluate the performance of the caching system, we focus on the probability that mobile users (MU) can successfully download their requested files from the SBSs, namely, successfully downloading probability (SDP). We develop the SDP expression based on the stochastic geometry theory. Since the derived SDP expression is complicated, we propose a simplified formulation of the SDP with the help of mathematical approximations. Furthermore, we investigate the impacts of the parameters of the SBSs, i.e., transmission power and deployment intensity, on the SDP. Monte-Carlo simulations are shown to be consistent with our derived SDP expressions. Numerical results also validate our analysis on the impacts of the related parameters on the SDP.

The rest of the paper is organized as follows. We first describe the system model in Section II and discuss the random caching process in Section III. Then we conduct the performance analysis of the proposed caching strategy in Section IV. Our simulations and numerical results are provided in Section V, and conclusions are summarized in Section VI.

II. SYSTEM MODEL

A. NETWORK MODEL

Let us consider a cellular network consisting of multiple MUs and SBSs that are operating on the same frequency spectrum. We model the distributions of the SBSs and the MUs as two independent homogeneous Poisson point processes (HPPP) Φ and Ψ, with the intensities λ_s and λ_u, respectively. The transmission power of the SBSs is denoted by P. The path-loss function of the channel from an SBS to an MU is denoted by $\zeta(d)$, where d represents the distance between them. The multi-path fading is modeled as Rayleigh fading with unit power, and hence the channel power gain of the multi-path fading is denoted by $h \sim \exp(1)$. All channels are assumed to be independently and identically distributed (*i.i.d.*).

As well known, the standard path-loss function can be calculated as $\zeta(d) = d^{-\alpha}$. Empirically, the exponent α ranges from 2 to 5. Although this standard path-loss function has been widely adopted, it has some limitations, especially when analyzing the densely and randomly distributed SBSs. Thus, we will focus on another path-loss model in the following, which is more practical in real systems, distinguishing whether the path loss is the type of LoS or NLoS. According to 3GPP [16], when considering the impact of LoS/NLoS, the path-loss function is expressed as

$$\zeta(d) = \begin{cases} \zeta_{\mathrm{L}}(d) \triangleq A_1 d^{-\alpha_1}, & \text{for LoS,} \\ \zeta_{\mathrm{N}}(d) \triangleq A_2 d^{-\alpha_2}, & \text{otherwise,} \end{cases} \tag{1}$$

where A_1 and A_2 are the path losses at a reference distance $d = 1$ for the LoS and NLoS cases, respectively. Also, α_1 and α_2 are the exponents corresponding to the LoS and NLoS, respectively. Generally, we have $\alpha_1 < \alpha_2$, i.e., the path loss in LoS channels is smaller than that in the NLoS ones. The path-loss model in Eq. (1) is currently supported by 3GPP [16].

Denote by $\mathcal{L}$ the event that the path between a transmitter and a receiver is an LoS path. Typically, the probability of $\mathcal{L}$ is a monotonically decreasing function with respect to the distance d between them. According to 3GPP,

the LoS probability is represented by

$$\Pr(\mathcal{L}) = \begin{cases} 1 - \dfrac{d}{d_1}, & 0 < d \le d_1, \\ 0, & d > d_1, \end{cases} \tag{2}$$

where d_1 is a distance threshold. In the case $d \le d_1$, the probability of LoS is a linearly decreasing function of d. When $d > d_1$, the contribution of LoS to the path loss will disappear and the channels are considered to be NLoS. Furthermore, in the scenario where $d_1 = \infty$ and $\alpha_1 = \alpha$, the path-loss model defined in Eq. (1) degrades to the standard path-loss model.

B. CONTENT REQUEST MODEL

Assume that network contents are stored in the form of files. We consider a file library consisting of M popular files with the same size. We denote by $q = [q_m : m = 1, \cdots, M]$ the popularity vector, where q_m represents the probability that the m-th file is requested by the MUs. The vector q can be viewed as the request probability mass function (PMF) of the M files. According to [17], the request PMF of the files can be modeled as a Zipf distribution, and the request probability q_m is calculated as

$$q_m = \frac{\frac{1}{m^\tau}}{\sum_{i=1}^{M} \frac{1}{i^\tau}}, \tag{3}$$

where τ is the exponent of the Zipf distribution. A larger τ implies a more uneven popularity distribution among those files. From (3), the probability of requesting a particular popular file goes to zero as $M \to \infty$ when $\tau < 1$, while it converges to a constant value for $\tau > 1$.

Due to the limited storage, each SBS cannot cache the entire file library. Therefore, we assume that the library is partitioned into N non-overlapped subsets, referred to as file groups (FG). Each SBS can only cache one of these N FGs, while an FG can be stored by multiple SBSs. The scenario of FGs with overlapping subsets of files will be considered later, which will be compared to the non-overlapping scenario. We denote by $\mathcal{G}_n$ the n-th FG, $n \in \{1, \cdots, N\}$. The probability that an MU requests a file in file group $\mathcal{G}_n$, denoted by Q_n, is thus given by

$$Q_n = \sum_{l} q_l, \quad \forall l, \text{ s.t. the } l\text{-th file is in } \mathcal{G}_n. \tag{4}$$

III. RANDOM SMALL-CELL CACHING

The random caching strategy consists of two stages. In the first stage, namely, file placement stage, each SBS independently caches an FG, say $\mathcal{G}_n$, with a specified caching probability, denoted by S_n. Hence, from the perspective of the entire network, the fraction of the SBSs that caches $\mathcal{G}_n$ is on average equal to S_n. Since the distribution of SBSs in the network is modeled as an HPPP with the intensity of λ_s, according to the thinning theorem in HPPP [18], we can view the distribution of SBSs that cache $\mathcal{G}_n$ as a thinned HPPP with the intensity of $S_n\lambda_s$.

We assume that at a particular time instant an MU can only request one file, and hence the distribution of MUs who request the files in $\mathcal{G}_n$ can be modeled as a thinned HPPP with the intensity $Q_n\lambda_u$. We view the SBSs that cache $\mathcal{G}_n$ together with the MUs that request the files in $\mathcal{G}_n$ as the n-th tier of the network, denoted by Tier-n.

In the second stage, namely, file delivery stage, the MU that requests a file in $\mathcal{G}_n$ will associate with an SBS that caches $\mathcal{G}_n$, and then tries to download the file from it. Generally, each MU tends to associate with the SBS which can provide the strongest received signal strength (RSS). The RSS from an SBS depends on many factors, such as the transmission power of the SBS, the distance and channel status between the SBS and the MU. Since the transmissions powers of the SBSs are assumed to be the same, statistically the nearest SBS provides the strongest average RSS.

Therefore, in our paper, we assume that when an MU requests a file, it will associate with the nearest SBS that cache it. Furthermore, to guarantee the transmission quality, we assume that only when the received signal-to-interference-and-noise-ratio (SINR) at the MU is no lower than a pre-set threshold, say, δ, can the requested file be successfully downloaded.

IV. PERFORMANCE ANALYSIS

In this section, we develop the average probability of the event $\mathcal{D}$ that an MU can successfully download the requested file from its associated SBS in the random caching, namely, average successful download probability $\Pr(\mathcal{D})$.

A. RECEIVED SINR

To obtain $\Pr(\mathcal{D})$, we start from the probability that a *typical* MU in Tier-n, say, located at the origin, can successfully download the requested files from its associated SBS. According to Slyvnyak's Theorem [18], the received SINR γ_n at this typical MU from its nearest SBS in Tier-n can be formulated as

$$\gamma_n = \frac{P h_{x_0} \zeta(\|x_0\|)}{\sum_{x_j \in \Phi \setminus \{x_0\}} P h_{x_j} \zeta(\|x_j\|) + \sigma^2}, \tag{5}$$

where σ^2 denotes the Gaussian noise power at the MU, x_0 denotes the location of the serving SBS which is the nearest to the typical MU in Tier-n, and x_j denotes the location of the interfering SBSs in Φ. Also, h_{x_0} and h_{x_j} denote the corresponding power gains of the channel fading.

Let δ be the pre-set SINR threshold, i.e., the minimum SINR required for successful transmissions, and let $\mathcal{D}_n$ be the event that the typical MU in Tier-n can successfully download the requested file from its associated SBS. Then the probability of $\mathcal{D}_n$ can be formulated as

$$\Pr(\mathcal{D}_n) = \Pr(\gamma_n \ge \delta). \tag{6}$$

Based on the result of $\Pr(\mathcal{D}_n)$ in Tier-n, we obtain the average probability of the event $\mathcal{D}$ as

$$\Pr(\mathcal{D}) = \sum_{n=1}^{N} Q_n \cdot \Pr(\mathcal{D}_n). \tag{7}$$

We can see from Eq. (7) that $\Pr(\mathcal{D}_n)$ is the key to obtaining $\Pr(\mathcal{D})$. Therefore in the following, we focus on the analysis of $\Pr(\mathcal{D}_n)$.

Note that in the scenario, when the different FGs may have an overlapping subset of files, the probability $\Pr(\mathcal{D})$ still has the same formulation as Eq. (7). However, all the subscripts n in Eq. (7) should be changed to m, because we should consider both the request probability and the caching probability of each file $\mathcal{F}_m$, i.e., S_m and Q_m, instead of each FG $\mathcal{G}_n$. Therefore, in this scenario, the specific SBSs that cache $\mathcal{F}_m$ and the MUs that request $\mathcal{F}_m$ are viewed as Tier-m. Since the formulations of SINR and $\Pr(\mathcal{D})$ are the same, we omit the analysis for this scenario with overlapping subsets of files for brevity.

B. ANALYSIS OF $\Pr(\mathcal{D}_n)$

To simplify the notation, we define $z \triangleq \|x_0\|$ as the distance between the typical MU and its nearest SBS in Tier-n. Since in Tier-n the deployment intensity of SBSs is $S_n\lambda_s$, and the number of the SBSs k in an area of A follows the Poisson distribution, the probability of the event that there is no SBS in the area with the radius of z can be calculated as [18]

$$\begin{aligned}\Pr(k = 0 \mid A = \pi z^2) &= e^{-AS_n\lambda_s}\frac{(AS_n\lambda_s)^k}{k!} \\ &= e^{-\pi z^2 S_n\lambda_s}.\end{aligned} \tag{8}$$

By using the derivative of (8), we can obtain the probability density function (PDF) of z, denoted by $f_n(z)$, as $f_n(z) = 2\pi S_n\lambda_s z\exp(-\pi S_n\lambda_s z^2)$.

Based on Eq. (6), the probability that the typical MU can successfully download the requested file in $\mathcal{G}_n$ can be calculated as

$$\begin{aligned}\Pr(\mathcal{D}_n) &= \mathbb{E}\left[1(\gamma_n(z) \geq \delta)\right] \\ &= \int_0^{\infty} \mathbb{E}_{h_{x_0},I}\left[1\left(\frac{\zeta(z)h_{x_0}}{I+\frac{\sigma^2}{P}} \geq \delta\right)\right] f_n(z)\mathrm{d}z,\end{aligned} \tag{9}$$

where I is defined as $I \triangleq \sum_{x_j\in\Phi\setminus\{x_0\}} h_{x_j}\zeta(\|x_j\|)$, $1(\cdot)$ is the indictor function, and $\mathbb{E}_X[\cdot]$ denotes the expectation over the variable X. As for the calculation of $\mathbb{E}_{h_{x_0},I}\left[1\left(\frac{\zeta(z)h_{x_0}}{I+\frac{\sigma^2}{P}} \geq \delta\right)\right]$ in (9), by applying the distribution of h_{x_0}, i.e., $h_{x_0} \sim \exp(1)$, we have

$$\begin{aligned}&\mathbb{E}_{h_{x_0},I}\left[1\left(\frac{\zeta(z)h_{x_0}}{I+\frac{\sigma^2}{P}} \geq \delta\right)\right] \\ &= \exp\left(-\frac{\delta\sigma^2}{P\zeta(z)}\right)\mathbb{E}_I\left[\exp\left(-\frac{\delta I}{\zeta(z)}\right)\right] \\ &= \exp\left(-\frac{\delta\sigma^2}{P\zeta(z)}\right)\mathscr{L}_I\left(\frac{\delta}{\zeta(z)}\right),\end{aligned} \tag{10}$$

where $\mathscr{L}_I(\kappa)$ is the Laplace transform of the random variable I evaluated at κ.

Based on the path-loss model in Eq. (1) and Eq. (2), the calculation of $\Pr(\mathcal{D}_n)$ in (9) contains three parts: 1) When $z \leq d_1$ and the LoS path happens with the probability $\Pr(\mathcal{L})$; 2) When $z \leq d_1$ and the NLoS path happens with the probability $1-\Pr(\mathcal{L})$; 3) When $z > d_1$ and only NLoS path exists. Substituting (1) and (2) into (9), we have

$$\begin{aligned}&\Pr(\mathcal{D}_n) \\ &= \int_0^{d_1} \mathbb{E}_{h_{x_0},I}\left[1\left(\frac{\zeta_L(z)h_{x_0}}{I+\frac{\sigma^2}{P}} \geq \delta\right)\right]\left(1-\frac{z}{d_1}\right) f_n(z)\mathrm{d}z \\ &\quad + \int_0^{d_1} \mathbb{E}_{h_{x_0},I}\left[1\left(\frac{\zeta_N(z)h_{x_0}}{I+\frac{\sigma^2}{P}} \geq \delta\right)\right]\frac{z}{d_1} f_n(z)\mathrm{d}z \\ &\quad + \int_{d_1}^{\infty} \mathbb{E}_{h_{x_0},I}\left[1\left(\frac{\zeta_N(z)h_{x_0}}{I+\frac{\sigma^2}{P}} \geq \delta\right)\right] f_n(z)\mathrm{d}z.\end{aligned} \tag{11}$$

According to Eq. (10), we need to calculate $\mathscr{L}_I\left(\frac{\delta}{\zeta_L(z)}\right)$ and $\mathscr{L}_I\left(\frac{\delta}{\zeta_N(z)}\right)$ for Eq. (11). In the case $z \leq d_1$, the received signal, as well as the interference, comes from both the LoS paths and the NLoS paths.

In the case $z > d_1$, the received signal, as well as the interference incurred by the SBSs of the same tier, comes only from the NLoS paths, while the interference incurred by other tiers comes from both the LoS paths and the NLoS paths. Based on the range of z, we have the following theorem regarding $\mathscr{L}_I\left(\frac{\delta}{\zeta_L(z)}\right)$ and $\mathscr{L}_I\left(\frac{\delta}{\zeta_N(z)}\right)$.

Theorem 1: In the range of $0 < z \leq d_1$, $\mathscr{L}_I\left(\frac{\delta}{\zeta(z)}\right)$ can be calculated by

$$\begin{aligned}&\mathscr{L}_I\left(\frac{\delta}{\zeta(z)}\right) \\ &= \exp\left(-\lambda_s 2\pi\left(\Theta_1\left(\alpha_1, 1, \frac{\zeta(z)}{\delta A_1}, d_1\right)\right.\right. \\ &\quad \left.\left. -\frac{1}{d_1}\Theta_1\left(\alpha_1, 2, \frac{\zeta(z)}{\delta A_1}, d_1\right)\right)\right) \\ &\quad \times \exp\left(-\lambda_s 2\pi\left(\frac{1}{d_1}\Theta_1\left(\alpha_2, 2, \frac{\zeta(z)}{\delta A_2}, d_1\right)\right.\right. \\ &\quad \left.\left. + \Theta_2\left(\alpha_2, 1, \frac{\zeta(z)}{\delta A_2}, d_1\right)\right)\right) \\ &\quad \times \exp\left(S_n\lambda_s 2\pi\left(\Theta_1\left(\alpha_1, 1, \frac{\zeta(z)}{\delta A_1}, z\right)\right.\right. \\ &\quad \left.\left. -\frac{1}{d_1}\Theta_1\left(\alpha_1, 2, \frac{\zeta(z)}{\delta A_1}, z\right) + \frac{1}{d_1}\Theta_1\left(\alpha_2, 2, \frac{\zeta(z)}{\delta A_2}, z\right)\right)\right).\end{aligned} \tag{12}$$

Here, $\zeta(z)$ can be either $\zeta_L(z)$ or $\zeta_N(z)$.

On the other hand, in the range of $z > d_1$, since the received signal only contains the NLoS part, we have

$$\mathscr{L}_I\left(\frac{\delta}{\zeta(z)}\right) = \mathscr{L}_I\left(\frac{\delta}{\zeta_N(z)}\right), \tag{13}$$

which can be calculated by

$$\begin{aligned}
&\mathscr{L}_I\left(\frac{\delta}{\zeta_N(z)}\right)\\
&= \exp\left(-\lambda_s 2\pi\left(\Theta_2\left(\alpha_2, 1, \frac{\zeta_N(z)}{\delta A_2}, d_1\right)\right)\right)\\
&\quad\times \exp\Bigg(-(1-S_n)\lambda_s 2\pi\Bigg(\Bigg(\Theta_1\left(\alpha_1, 1, \frac{\zeta_N(z)}{\delta A_1}, d_1\right)\\
&\quad- \frac{1}{d_1}\Theta_1\left(\alpha_1, 2, \frac{\zeta_N(z)}{\delta A_1}, d_1\right)\\
&\quad+ \frac{1}{d_1}\Theta_1\left(\alpha_2, 2, \frac{\zeta_N(z)}{\delta A_2}, d_1\right)\Bigg)\Bigg)\\
&\quad\times \exp\left(S_n\lambda_s 2\pi\left(\Theta_1\left(\alpha_2, 1, \frac{\zeta_N(z)}{\delta A_2}, z\right)\right.\right.\\
&\quad\left.\left.- \Theta_1\left(\alpha_2, 1, \frac{\zeta_N(z)}{\delta A_2}, d_1\right)\right)\right). \qquad (14)
\end{aligned}$$

In Eqs. (12) and (14), we have

$$\begin{aligned}
&\Theta_1(\alpha, \beta, u, d)\\
&\quad\triangleq \int_0^d \frac{r^\beta}{1+ur^\alpha}\mathrm{d}r\\
&\quad= \frac{d^{(\beta+1)}}{\beta+1}{}_2F_1\left(1, \frac{\beta+1}{\alpha}; 1+\frac{\beta+1}{\alpha}; -ud^\alpha\right), \qquad (15)
\end{aligned}$$

and

$$\begin{aligned}
&\Theta_2(\alpha, \beta, u, d)\\
&\triangleq \int_d^\infty \frac{r^\beta}{1+ur^\alpha}\mathrm{d}r = \frac{d^{-(\alpha-\beta-1)}}{u(\alpha-\beta-1)}\\
&\quad\times{}_2F_1\left(1, 1-\frac{\beta+1}{\alpha}; 2-\frac{\beta+1}{\alpha}; -\frac{1}{ud^\alpha}\right), (\alpha > \beta+1), \qquad (16)
\end{aligned}$$

where ${}_2F_1(\cdot,\cdot;\cdot;\cdot)$ represents the hyper-geometric function.

Proof: Please refer to Appendix A.

From the above analysis, by substituting Eqs. (12), (14) and (10) into Eq. (11), we can thus obtain the analytical result of $\Pr(\mathcal{D}_n)$.

C. DISCUSSIONS ON PARAMETERS

1) TRANSMISSION POWER P

We analyze the impact of the power P on $\Pr(\mathcal{D}_n)$, and have the following remark.

Remark 1: From *Theorem 1*, we can see that $\mathscr{L}_I(\kappa)$ is independent of the transmission power P. Further combined with Eq. (10), we conclude that $\Pr(\mathcal{D}_n)$ increases with the enhancement of P. However, when P is large enough, the item $\exp\left(-\frac{\delta\sigma^2}{P\zeta(z)}\right)$ in Eq. (10) approaches to one. In this case, $\Pr(\mathcal{D}_n)$ converges to a constant in terms of P.

2) DISTANCE THRESHOLD d_1

We consider two limit cases of the distance threshold d_1, namely $d_1 \to 0$ and $d_1 \to \infty$. Both cases can be viewed as the standard path-loss model. In the case $d_1 \to 0$, only NLoS paths present and LoS paths will disappear, and the path-loss function can be written as $\zeta(d) = d^{-\alpha_2}$. In the case $d_1 \to \infty$, only LoS paths present and NLoS paths will disappear, and the path-loss function is $\zeta(d) = d^{-\alpha_1}$. We have the following theorem.

Theorem 2: For the two limit cases of d_1, the probability $\Pr(\mathcal{D}_n)$ can be expressed as

$$\begin{aligned}
&\lim_{d_1\to 0}\Pr(\mathcal{D}_n)\\
&= \int_0^\infty \pi S_n\lambda_s \exp\left(-\frac{z^{\alpha_2}\delta\sigma^2}{P}\right)\\
&\quad\times \exp\left(-\pi\lambda_s z^2((1-S_n)C(\delta,\alpha_2) + S_nA(\delta,\alpha_2)+S_n)\right)\mathrm{d}z^2, \qquad (17)
\end{aligned}$$

and

$$\begin{aligned}
&\lim_{d_1\to\infty}\Pr(\mathcal{D}_n)\\
&= \int_0^\infty \pi S_n\lambda_s \exp\left(-\frac{z^{\alpha_1}\delta\sigma^2}{P}\right)\\
&\quad\times \exp\left(-\pi\lambda_s z^2((1-S_n)C(\delta,\alpha_1) + S_nA(\delta,\alpha_1)+S_n)\right)\mathrm{d}z^2, \qquad (18)
\end{aligned}$$

where $A(\delta,\alpha) \triangleq \delta\frac{2}{\alpha-2}\ {}_2F_1\left(1, 1-\frac{2}{\alpha}; 2-\frac{2}{\alpha}; -\delta\right)$, and $C(\delta,\alpha) \triangleq \frac{2}{\alpha}\delta^{\frac{2}{\alpha}}B\left(\frac{2}{\alpha}, 1-\frac{2}{\alpha}\right)$. Furthermore, $B(\cdot)$ represents the beta function.

Proof: Please refer to Appendix B.

Considering $d_1 \to 0$, when the transmission power P goes to infinity, the item $\exp\left(-\frac{z^{\alpha_2}\delta\sigma^2}{P}\right)$ in Eq. (17), approaches one. Then we have the closed form of $\Pr(\mathcal{D}_n)$ as

$$\lim_{d_1\to 0, P\to\infty}\Pr(\mathcal{D}_n) = \frac{S_n}{(1-S_n)C(\delta,\alpha_2) + S_nA(\delta,\alpha_2) + S_n}. \qquad (19)$$

Similarly, we can obtain $\lim_{d_1, P\to\infty}\Pr(\mathcal{D}_n)$ by replacing α_2 in Eq. (19) with α_1.

Remark 2: From above discussions, when $d_1 \to 0$ (or $d_1 \to \infty$) and $P \to \infty$, the probability $\Pr(\mathcal{D}_n)$ is independent of the deployment intensity λ_s.

D. SIMPLIFIED EXPRESSION VIA APPROXIMATIONS

For those general cases $0 < d_1 < \infty$, the results in *Theorem 2* are not applicable. At the same time, the expression of $\Pr(\mathcal{D}_n)$ in Eq. (11) is quite complicated, and thus cannot provide insightful results for a better understanding of $\Pr(\mathcal{D}_n)$. In this subsection, we will focus on how to obtain a simplified form of $\Pr(\mathcal{D}_n)$ via some approximations. First, we can neglect the third item of Eq. (11), since signals ranged from z to infinity is quite weak compared with that ranged from 0 to z. Second, we can further neglect the second item, since signals from the NLoS paths is quite weak compared with those from the LoS paths. Therefore, $\Pr(\mathcal{D}_n)$ in Eq. (11) can be approximated as

$$\begin{aligned}
\Pr(\mathcal{D}_n) \approx \int_0^{d_1} &\mathbb{E}_{h_{x_0}, I}\left[1\left(\frac{\zeta_L(z)h_{x_0}}{I+\frac{\sigma^2}{P}} \geq \delta\right)\right]\\
&\times\left(1-\frac{z}{d_1}\right)f_n(z)\mathrm{d}z. \qquad (20)
\end{aligned}$$

Next, we observe the expression of $\mathscr{L}_I\left(\frac{\delta}{\zeta(z)}\right)$ in Eq. (12). According to (15) and (16), we can see that both $\Theta_1(\alpha,\beta,u,d)$ and $\Theta_2(\alpha,\beta,u,d)$ decrease exponentially with the increase of α. Since we have $\alpha_2 > \alpha_1$, we neglect those items in Eq. (12) that contain α_2 as a parameter. Therefore, $\mathscr{L}_I\left(\frac{\delta}{\zeta_L(z)}\right)$ can be approximated as

$$\begin{aligned}\mathscr{L}_I\left(\frac{\delta}{\zeta_L(z)}\right) \approx \exp\Bigg(-\lambda_s 2\pi\Bigg(&\Theta_1\left(\alpha_1,1,\frac{\zeta_L(z)}{\delta A_1},d_1\right)\\ &-\frac{1}{d_1}\Theta_1\left(\alpha_1,2,\frac{\zeta_L(z)}{\delta A_1},d_1\right)\Bigg)\Bigg)\\ \times\exp\Bigg(S_n\lambda_s 2\pi\Bigg(&\Theta_1\left(\alpha_1,1,\frac{\zeta_L(z)}{\delta A_1},z\right)\\ &-\frac{1}{d_1}\Theta_1\left(\alpha_1,2,\frac{\zeta_L(z)}{\delta A_1},z\right)\Bigg)\Bigg).\end{aligned} \tag{21}$$

By substituting Eq. (21) into Eq. (20), we can obtain the simplified expression of $\Pr(\mathcal{D}_n)$. Compared with the exact calculation of $\Pr(\mathcal{D}_n)$ in Subsection B, the above approximation on $\Pr(\mathcal{D}_n)$ can dramatically reduce the calculation complexity by two thirds.

E. FURTHER ANALYSIS WITH A SPECIAL CASE $\alpha_1 = 2$

As we have simplified the expression of $\Pr(\mathcal{D}_n)$, we will further consider the approximations in the following special case. According to 3GPP [16], the practical value of the LoS parameter α_1 is 2.09. Therefore, in the following analysis, we set $\alpha_1 = 2$ for simplicity. First, according to the definition of Θ_1 in Eq. (15), we have

$$\begin{aligned}\Theta_1\left(\alpha_1=2,1,\frac{\zeta_L(z)}{\delta A_1},d_1\right) &= \frac{d_1^2}{2}{}_2F_1\left(1,1;2;-\frac{d_1^2}{\delta z^2}\right)\\ &= \frac{\delta z^2}{2}\ln\left(1+\frac{d_1^2}{\delta z^2}\right).\end{aligned} \tag{22}$$

Similarly, we have

$$\Theta_1\left(\alpha_1=2,1,\frac{\zeta_L(z)}{\delta A_1},z\right) = \frac{\delta z^2}{2}\ln\left(1+\frac{1}{\delta}\right). \tag{23}$$

Then we focus on

$$\Theta_1\left(\alpha_1=2,2,\frac{\zeta_L(z)}{\delta A_1},d_1\right) = \frac{d_1^3}{3}{}_2F_1\left(1,\frac{3}{2};\frac{5}{2};-\frac{d_1^2}{\delta z^2}\right). \tag{24}$$

According to the properties of the hyper-geometric function, the following two equations hold:

$$\begin{aligned}{}_2F_1\left(1,\frac{3}{2};\frac{5}{2};-\frac{d_1^2}{\delta z^2}\right) &= \frac{3\delta z^2}{d_1^2}\left(1-{}_2F_1\left(1,\frac{1}{2};\frac{3}{2};-\frac{d_1^2}{\delta z^2}\right)\right),\\ {}_2F_1\left(1,\frac{1}{2};\frac{3}{2};-\frac{d_1^2}{\delta z^2}\right) &= \frac{\sqrt{\delta}z}{d_1}\arctan\left(\frac{d_1}{\sqrt{\delta}z}\right).\end{aligned} \tag{25}$$

By combining Eqs. (24) and (25), we can then obtain

$$\Theta_1\left(\alpha_1=2,2,\frac{\zeta_L(z)}{\delta A_1},d_1\right) = \delta z^2 d_1 - \delta\sqrt{\delta}z^3\arctan\left(\frac{d_1}{\sqrt{\delta}z}\right). \tag{26}$$

Similarly, there is

$$\Theta_1\left(\alpha_1=2,2,\frac{\zeta_L(z)}{\delta A_1},z\right) = \delta z^3 - \delta\sqrt{\delta}z^3\arctan\left(\frac{1}{\sqrt{\delta}}\right). \tag{27}$$

Based on the above discussions, we can rewrite Eq. (21) with the closed-form as

$$\begin{aligned}&\mathscr{L}_I\left(\frac{\delta}{\zeta_L(z)}\right)\\ &= \exp\Bigg\{-\lambda_s 2\pi\Bigg(\frac{\delta z^2}{2}\ln\left(1+\frac{d_1^2}{\delta z^2}\right)-\delta z^2\\ &\quad+\delta\sqrt{\delta}\frac{z^3}{d_1}\arctan\left(\frac{d_1}{\sqrt{\delta}z}\right)-\frac{S_n\delta z^2}{2}\ln\left(1+\frac{1}{\delta}\right)\\ &\quad+\frac{S_n\delta z^3}{d_1}-S_n\delta\sqrt{\delta}\frac{z^3}{d_1}\arctan\left(\frac{1}{\sqrt{\delta}}\right)\Bigg)\Bigg\}.\end{aligned} \tag{28}$$

V. NUMERICAL RESULTS

In this section, we present numerical and Monte-Carlo simulation results of $\Pr(\mathcal{D})$ versus various parameters. In the Monte-Carlo simulations, the performance is averaged over 500 network cases, and in each case SBSs and MUs are randomly distributed in an area of $5 \times 5\text{km}^2$ according to HPPP. Unless otherwise specified, the parameters throughout this section are arranged as follows. First, to comply with the 3GPP standards [16], the transmission power and the noise power are set to $P = 30$dBm (i.e., 1 Watt) and $\sigma^2 = -95$dBm (i.e., $10^{-12.5}$ Watts), respectively. Second, the parameters related to the path-loss model also comply with [16]. To be specific, we set $\alpha_1 = 2.09$, $A_1 = 10^{-10.38}$, $\alpha_2 = 3.75$, and $A_2 = 10^{-14.54}$. Also, we set the distance threshold to $d_1 = 0.3$km.

Regarding the intensity of the HPPP distributed SBSs, we have $\lambda_s = 100/\text{km}^2$, representing that there are on average 100 SBSs per kilometer square. Additionally, we consider a file library consisting of $M = 100$ files, which is divided into $N = 5$ file groups, i.e., each SBS stores 20 files. The Zipf exponent is set as $\tau = 1.4$. We consider a simple grouping strategy that the m-th file belongs to the FG $\mathcal{G}_n$ if $m \in \left[\frac{M}{N}(n-1)+1,\cdots,\frac{M}{N}n\right]$, $\forall n \in \{1,\cdots,N\}$. Note that, the way on packing which files into a group does not affect our theoretical derivations, since it only changes the values of the request PMF $\{Q_n\}$. For the caching probability, we set $S_n = Q_n$.

In all the following figures, three SINR thresholds are investigated, i.e., $\delta = -3$dB, -6dB, and -10dB. Fig. 2 shows the numerical (solid-line) and simulation results (dashed-line) of $\Pr(\mathcal{D})$ when the transmission power of SBSs grows from -40dBm to 40dBm. Note that the numerical results are obtained based on the analysis in Subsection B of Section IV. We can see that our analytical results are highly consistent with the simulation ones. A smaller δ leads to a higher $\Pr(\mathcal{D})$. Also, it is shown that $\Pr(\mathcal{D})$ increases monotonically with P. In particular, when P is in the range from -40dBm to 0dBm, $\Pr(\mathcal{D})$ increases dramatically with P.

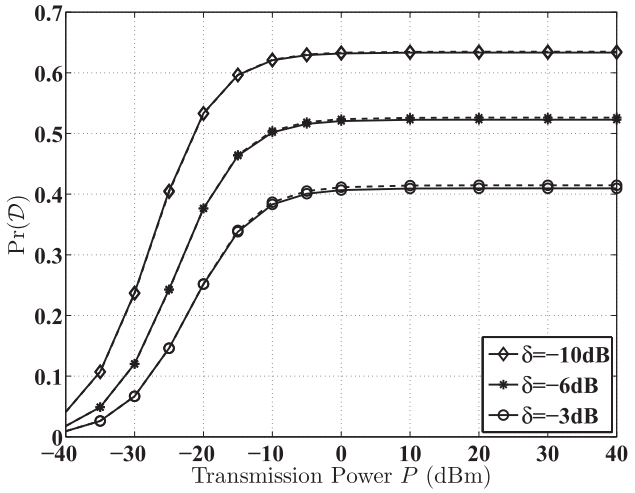

FIGURE 2. The numerical and simulation results of Pr($\mathcal{D}$) versus various values of transmission power. The solid-line represents the analytical results, and the dashed-line represents the Monte-Carlo simulations.

On the other hand, when P is large enough, say, $P \geq 10$dBm, further increasing P will not improve Pr($\mathcal{D}$). These phenomena are consistent with our discussions in *Remark 1*.

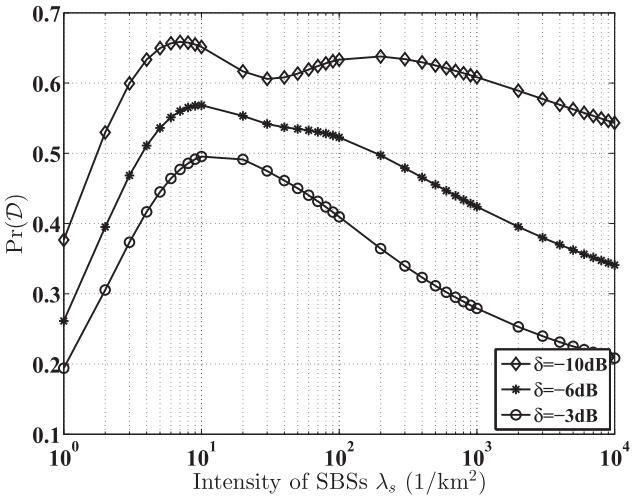

FIGURE 3. The performance of Pr($\mathcal{D}$) versus various values of λ_s.

After verifying our analytical results by Monte-Carlo simulations, in the following, we only discuss the performance of Pr($\mathcal{D}$) based on the analytical results. Fig. 3 shows the Pr($\mathcal{D}$) versus various values of λ_s. Roughly speaking, Pr($\mathcal{D}$) first increases and then drops down with the increase of λ_s. However, Pr($\mathcal{D}$) is not always a convex function of λ_s, as there are saddles that can be seen in the curves. In contrast, Fig. 4 plots the standard path-loss model when d_1 approaches 0, i.e., only NLoS remains, based on Eq. (17). It is shown that Pr($\mathcal{D}$) first increases and then keeps constant in terms of λ_s. Three power levels are investigated, i.e., $P = 10$dBm (dashed-line), $P = 30$dBm (dotted-line), and $P = 50$dBm (solid-line). We can see that when P is large enough, Pr($\mathcal{D}$) will be independent of λ_s. This verifies our discussions in *Remark 2*.

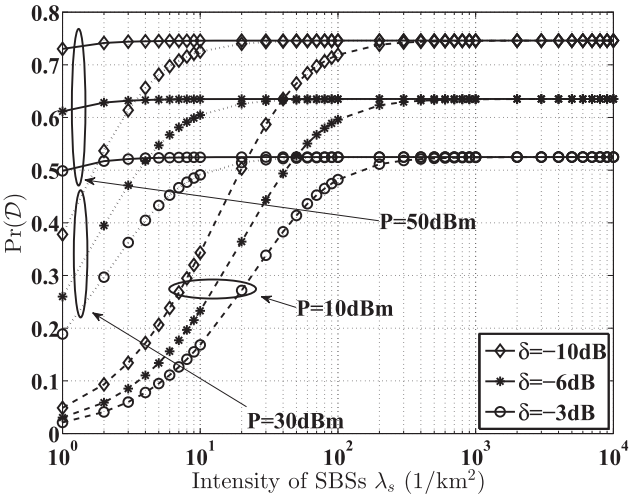

FIGURE 4. The performance of Pr($\mathcal{D}$) versus various values of λ_s for there standard path-loss model, where we have $d_1 \to 0$. Three power levers are investigated, i.e., $P = 10$dBm (dashed-line), $P = 30$dBm (dotted-line), and $P = 50$dBm (solid-line).

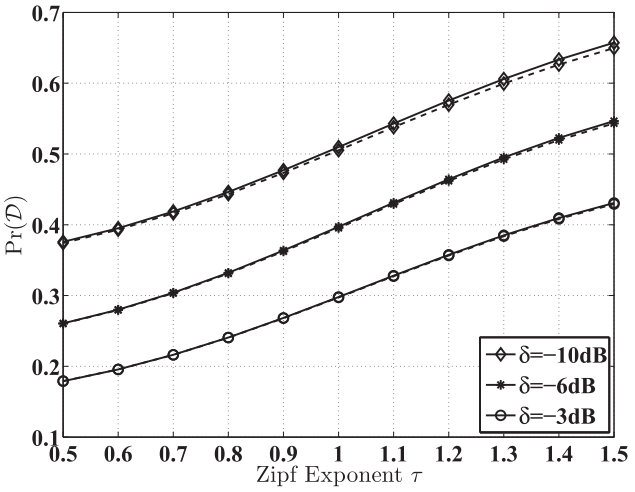

FIGURE 5. The performance of Pr($\mathcal{D}$) versus the file popularity exponent τ. The solid-line represents the exact results, while the dashed-line represents the approximated results.

Fig. 5 shows the impact of the file popularity parameter τ on Pr($\mathcal{D}$), where the solid-line represents the results for the exact calculation of Pr($\mathcal{D}$), while the dashed-line represents the approximated ones obtained by Eq. (20). First, it is shown that the approximated calculation on Pr($\mathcal{D}$) derived is highly constant with the exact one. Furthermore, we can see from the figure that when the exponent of Zipf distribution increases, Pr($\mathcal{D}$) increases accordingly. This means that a more uneven popularity among the files will further improve the successful download probability. We also investigate the impact of the storage size of the SBSs on the performance.

Fig. 6 shows the performance of Pr($\mathcal{D}$) versus various storage sizes. Again, it is shown that the approximate Pr($\mathcal{D}$) matches the exact one. Furthermore, a large storage size helps to increase the successful download probability.

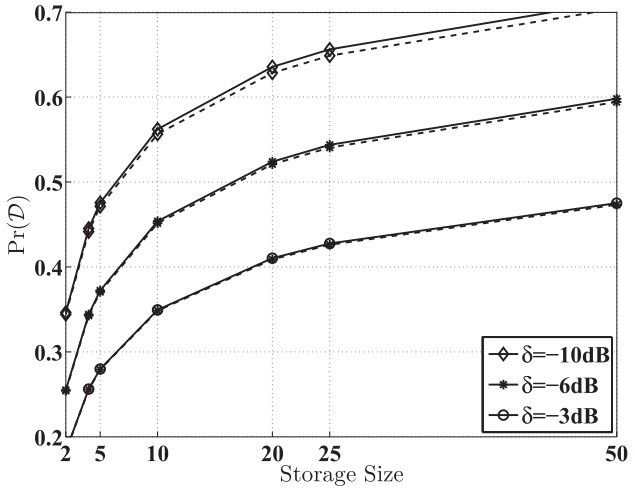

FIGURE 6. The performance of Pr($\mathcal{D}$) versus various storage size, i.e, the number of files in each FG. The solid-line represents the exact results, while the dashed-line represents the approximated results. We consider the following storage size: 2, 5, 10, 20, 25 and 50. Correspondingly, there are 50, 20, 10, 5, 4 and 2 FGs.

VI. CONCLUSIONS

In this paper, we analyzed the performance of a random caching strategy considering the impact of LoS and NLoS and the HPPP distributed SBSs based on stochastic geometry theory. Specifically, we analyzed the probability of the event that an MU can successfully download its requested files from the storage of the associated SBSs, i.e., Pr($\mathcal{D}$). The impacts of P and λ_s on this probability was also investigated. From the analysis and simulations, we concluded that increasing the SBSs' transmission power P is helpful to improve the successful download probability. However, Pr($\mathcal{D}$) keeps constant when P is large enough. Also, there exists an optimal λ_s to maximize the successful download probability. However, in the standard path-loss model, when P is large enough, the Pr($\mathcal{D}$) will be independent of λ_s. Finally, we showed that a larger disparity among the files' popularity and a larger storage size will improve the performance.

APPENDIX A
PROOF OF *THEOREM 1*

According to [18], we have

$$\begin{aligned}\mathscr{L}_I(\kappa) &= \mathbb{E}_I\left[\exp\left(-\kappa I\right)\right]\\ &= \mathbb{E}_I\left[\exp\left(-\kappa\sum_{x_j\in\Phi\setminus\{x_0\}} h_{x_j}\zeta(\|x_j\|)\right)\right]\\ &= \mathbb{E}_{h_{x_j},x_j}\left[\prod_{x_j\in\Phi\setminus\{x_0\}}\exp\left(-\kappa\zeta(\|x_j\|)h_{x_j}\right)\right]\\ &= \mathbb{E}_{x_j}\left[\prod_{x_j\in\Phi\setminus\{x_0\}}\frac{1}{1+\kappa\zeta(\|x_j\|)}\right]\\ &= \exp\left(-\lambda_s 2\pi\int_0^\infty\left(1-\frac{1}{1+\kappa\zeta(r)}\right)r\mathrm{d}r\right.\\ &\quad\left.+S_n\lambda_s 2\pi\int_0^z\left(1-\frac{1}{1+\kappa\zeta(r)}\right)r\mathrm{d}r\right),\end{aligned}\tag{29}$$

where to simplify the notation, we use $r \triangleq \|x_j\|$. The interference I comes from two parts: the SBSs in other tiers which locate in the entire area of the network, and the SBSs in the n-th tier whose distances with the typical MU are larger than z. Since distribution of the SBSs in other tiers can be viewed as an HPPP with intensity $(1-S_n)\lambda_s$.

The first integral of (Eq. 29) can be calculated as

$$\begin{aligned}&\int_0^\infty\left(1-\frac{1}{1+\kappa\zeta(r)}\right)r\mathrm{d}r\\ &=\int_0^{d_1}\left(1-\frac{1}{1+\kappa\zeta_L(r)}\right)\\ &\quad\times r\Pr(\mathcal{L})\mathrm{d}r+\int_{d_1}^\infty\left(1-\frac{1}{1+\kappa\zeta_N(r)}\right)r\mathrm{d}r\\ &\quad+\int_0^{d_1}\left(1-\frac{1}{1+\kappa\zeta_N(r)}\right)r(1-\Pr(\mathcal{L}))\mathrm{d}r.\end{aligned}\tag{30}$$

After some manipulations, we arrive at

$$\begin{aligned}&\int_0^\infty\left(1-\frac{1}{1+\kappa\zeta(r)}\right)r\mathrm{d}r\\ &=\int_0^{d_1}\left(\frac{1}{1+(\kappa A_1)^{-1}r^{\alpha_1}}\right)r\mathrm{d}r\\ &\quad-\int_0^{d_1}\left(\frac{1}{1+(\kappa A_1)^{-1}r^{\alpha_1}}+\frac{1}{1+(\kappa A_2)^{-1}r^{\alpha_2}}\right)\frac{r^2}{d_1}\mathrm{d}r\\ &\quad+\int_{d_1}^\infty\left(\frac{1}{1+(\kappa A_2)^{-1}r^{\alpha_2}}\right)r\mathrm{d}r=\Theta_1\left(\alpha_1,1,(\kappa A_1)^{-1},d_1\right)\\ &\quad-\frac{1}{d_1}\Theta_1(\alpha_1,2,(\kappa A_1)^{-1},d_1)+\frac{1}{d_1}\Theta_1(\alpha_2,2,(\kappa A_2)^{-1},d_1)\\ &\quad+\Theta_2(\alpha_2,1,(\kappa A_2)^{-1},d_1).\end{aligned}\tag{31}$$

For the second integral of Eq. (29), in the case $z\in(0,d_1)$, we have

$$\begin{aligned}&\int_0^z\left(1-\frac{1}{1+\kappa\zeta(r)}\right)r\mathrm{d}r\\ &=\int_0^z\left(\frac{\kappa\zeta_{\mathrm{L}}(r)}{1+\kappa\zeta_{\mathrm{L}}(r)}\right)r\Pr(\mathcal{L})\mathrm{d}r\\ &\quad+\int_0^z\left(\frac{\kappa\zeta_{\mathrm{N}}(r)}{1+\kappa\zeta_{\mathrm{N}}(r)}\right)r(1-\Pr(\mathcal{L}))\mathrm{d}r\\ &=\Theta_1(\alpha_1,1,(\kappa A_1)^{-1},z)-\frac{1}{d_1}\Theta_1(\alpha_1,2,(\kappa A_1)^{-1},z)\\ &\quad+\frac{1}{d_1}\Theta_1(\alpha_2,2,(\kappa A_2)^{-1},z).\end{aligned}\tag{32}$$

Furthermore, when $z>d_1$, we have

$$\begin{aligned}&\int_0^z\left(1-\frac{1}{1+\kappa\zeta(r)}\right)r\mathrm{d}r\\ &=\int_0^{d_1}\left(1-\frac{1}{1+\kappa\zeta_{\mathrm{L}}(r)}\right)r\Pr(\mathcal{L})\mathrm{d}r\end{aligned}$$

$$+\int_{d_1}^{z}\left(1-\frac{1}{1+\kappa\zeta_{\mathrm{N}}(r)}\right)r\mathrm{d}r$$
$$+\int_{0}^{d_1}\left(1-\frac{1}{1+\kappa\zeta_{\mathrm{N}}(r)}\right)r(1-\Pr(\mathcal{L}))\mathrm{d}r$$
$$=\Theta_1(\alpha_1,1,(\kappa A_1)^{-1},d_1)-\frac{1}{d_1}\Theta_1\left(\alpha_1,2,(\kappa A_1)^{-1},\ d_1\right)$$
$$+\frac{1}{d_1}\Theta_1(\alpha_2,2,(\kappa A_2)^{-1},d_1)$$
$$+\Theta_1(\alpha_2,1,(\kappa A_2)^{-1},z)-\Theta_1(\alpha_2,1,(\kappa A_2)^{-1},d_1). \quad (33)$$

This completes the proof. ■

APPENDIX B
PROOF OF *THEOREM 2*

When d_1 goes to infinity, $\Pr(\mathcal{D}_n)$ in Eq. (11) can be rewritten as

$$\Pr(\mathcal{D}_n)=\int_0^{\infty}\mathbb{E}_{h_{x_0},I}\left[1\left(\frac{\zeta_L(z)h_{x_0}}{I+\frac{\sigma^2}{P}}\geq\delta\right)\right]f_n(z)\mathrm{d}z$$
$$=\int_0^{\infty}\mathbb{E}_I\left[\exp\left(-z^{\alpha_1}\delta I\right)\right]$$
$$\times\exp\left(-\frac{z^{\alpha_1}\delta\sigma^2}{P}\right)2\pi S_n\lambda_s z\exp(-\pi S_n\lambda_s z^2)\mathrm{d}z. \quad (34)$$

For the item $\mathbb{E}_I\left[\exp\left(-z^{\alpha_1}\delta I\right)\right]$, we can follow a similar derivation method in Appendix A and let $d_1\to\infty$. Then we have

$$\mathbb{E}_I\left[\exp\left(-z^{\alpha_1}\delta I\right)\right]$$
$$=\exp\left(-2\pi\sum_{i=1,i\neq n}^{N}S_i\lambda_s\frac{1}{\alpha_1}\delta^{\frac{2}{\alpha_1}}\left(\frac{2}{\alpha_1},1-\frac{2}{\alpha_1}\right)z^2\right.$$
$$\left.-S_n\lambda_s\pi z^2\frac{2\delta}{\alpha_1-2}\,{}_2F_1\left(1,1-\frac{2}{\alpha_1};2-\frac{2}{\alpha_1};-\delta\right)\right). \quad (35)$$

By substituting Eq. (35) into Eq. (34), we obtain $\lim_{d_1\to\infty}\Pr(\mathcal{D}_n)$. By following the same method, we can find $\lim_{d_1\to 0}\Pr(\mathcal{D}_n)$ for the case $d_1\to 0$. This completes the proof. ■

REFERENCES

[1] J. Erman, A. Gerber, M. Hajiaghayi, D. Pei, S. Sen, and O. Spatscheck, "To cache or not to cache: The 3G case," *IEEE Internet Comput.*, vol. 15, no. 2, pp. 27–34, Mar./Apr. 2011.
[2] U. Niesen, D. Shah, and G. W. Wornell, "Caching in wireless networks," *IEEE Trans. Inf. Theory*, vol. 58, no. 10, pp. 6524–6540, Oct. 2012.
[3] X. Wang, M. Chen, T. Taleb, A. Ksentini, and V. C. M. Leung, "Cache in the air: Exploiting content caching and delivery techniques for 5G systems," *IEEE Commun. Mag.*, vol. 52, no. 2, pp. 131–139, Feb. 2014.
[4] E. Bastug, M. Bennis, and M. Debbah, "Living on the edge: The role of proactive caching in 5G wireless networks," *IEEE Commun. Mag.*, vol. 52, no. 8, pp. 82–89, Aug. 2014.
[5] E. Baştuğ, M. Bennis, M. Kountouris, and M. Debbah, "Cache-enabled small cell networks: Modeling and tradeoffs," *EURASIP J. Wireless Commun. Netw.*, vol. 2015, no. 1, p. 41, 2015.
[6] M. Maddah-Ali and U. Niesen, "Decentralized coded caching attains order-optimal memory-rate tradeoff," *IEEE/ACM Trans. Netw.*, vol. 23, no. 4, pp. 1029–1040, Aug. 2015.
[7] S. Woo, E. Jeong, S. Park, J. Lee, S. Ihm, and K. Park, "Comparison of caching strategies in modern cellular backhaul networks," in *Proc. 11th Annu. Int. Conf. Mobile Syst., Appl., Services*, New York, NY, USA, 2013, pp. 319–332.
[8] H. Ahlehagh and S. Dey, "Video-aware scheduling and caching in the radio access network," *IEEE/ACM Trans. Netw.*, vol. 22, no. 5, pp. 1444–1462, Oct. 2014.
[9] K. Shanmugam, N. Golrezaei, A. G. Dimakis, A. F. Molisch, and G. Caire, "FemtoCaching: Wireless content delivery through distributed caching helpers," *IEEE Trans. Inf. Theory*, vol. 59, no. 12, pp. 8402–8413, Dec. 2013.
[10] N. Golrezaei, A. F. Molisch, A. G. Dimakis, and G. Caire, "Femtocaching and device-to-device collaboration: A new architecture for wireless video distribution," *IEEE Commun. Mag.*, vol. 51, no. 4, pp. 142–149, Apr. 2013.
[11] M. Ji, G. Caire, and A. F. Molisch, "Wireless device-to-device caching networks: Basic principles and system performance," *IEEE J. Sel. Areas Commun.*, vol. 34, no. 1, pp. 176–189, Jan. 2015.
[12] N. Golrezaei, P. Mansourifard, A. F. Molisch, and A. G. Dimakis, "Base-station assisted device-to-device communications for high-throughput wireless video networks," *IEEE Trans. Wireless Commun.*, vol. 13, no. 7, pp. 3665–3676, Jul. 2014.
[13] H. J. Kang and C. G. Kang, "Mobile device-to-device (D2D) content delivery networking: A design and optimization framework," *J. Commun. Netw.*, vol. 16, no. 5, pp. 568–577, Oct. 2014.
[14] H. Zhang, X. Chu, W. Guo, and S. Wang, "Coexistence of WI-FI and heterogeneous small cell networks sharing unlicensed spectrum," *IEEE Commun. Mag.*, vol. 53, no. 3, pp. 158–164, Mar. 2015.
[15] K. Poularakis, G. Iosifidis, and L. Tassiulas, "Approximation algorithms for mobile data caching in small cell networks," *IEEE Trans. Commun.*, vol. 62, no. 10, pp. 3665–3677, Oct. 2014.
[16] "Evolved Universal Terrestrial Radio Access (E-UTRA) Further advancements for E-UTRA physical layer aspects," 3GPP, Tech. Rep. v.9.0.0, Mar. 2010. [Online]. Available: www.3gpp.org
[17] M. Zink, K. Suh, Y. Gu, and J. Kurose, "Characteristics of YouTube network traffic at a campus network—Measurements, models, and implications," *Comput. Netw.*, vol. 53, no. 4, pp. 501–514, Mar. 2009.
[18] D. Stoyan, W. Kendall, and J. Mecke, *Stochastic Geometry and its Applications*, 2nd ed. Hoboken, NJ, USA: Wiley, 1995.

JUN LI (M'09–SM'16) received the Ph.D. degree in electronic engineering from Shanghai Jiao Tong University, Shanghai, China, in 2009. In 2009, he was with the Department of Research and Innovation, Alcatel Lucent Shanghai Bell, as a Research Scientist. From 2009 to 2012, he was a Post-Doctoral Fellow with the School of Electrical Engineering and Telecommunications, The University of New South Wales, Australia. Since 2012, he has been a Research Fellow with the School of Electrical Engineering, The University of Sydney, Australia. His research interests include network information theory, channel coding theory, wireless network coding, and cooperative communications.

YOUJIA CHEN received the B.S. and M.S. degrees in communication engineering from Nanjing University, Nanjing, China, in 2005 and 2008, respectively. She is currently pursuing the Ph.D. degree in wireless engineering with The University of Sydney, Australia. From 2008 to 2009, she was with Alcatel-Lucent Shanghai Bell. Since 2009, she has been with the College of Photonic and Electrical Engineering, Fujian Normal University, China. Her current research interests include resource management, load balancing, and caching strategy in heterogeneous cellular networks.

MING DING (M'12) received the B.S. and M.S. degrees (Hons.) in electronics engineering and the Ph.D. degree in signal and information processing from Shanghai Jiao Tong University (SJTU), Shanghai, China, in 2004, 2007, and 2011, respectively. From 2007 to 2011, he was with Sharp Laboratories of China (SLC), SJTU, as a Researcher/Senior Researcher. He was with SLC as a Senior Researcher/Principal Researcher until 2014, when he joined National Information and Communications Technology Australia (NICTA). In 2015, Commonwealth Scientific and Industrial Research Organization and NICTA joined forces to create Data61, where he was a Senior Research Scientist with the Research and Development Center, Sydney, NSW, Australia. He has authored about 40 papers in IEEE journals and conferences, all in recognized venues, and about 20 3GPP standardization contributions, and the Springer book *Multi-point Cooperative Communication Systems: Theory and Applications*. He holds 15 CN, seven JP, three U.S., and two KR patents. He has co-authored over 100 patent applications on 4G/5G technologies.

FENG SHU (M'07) received the B.S. degree from the Fuyang Teaching College, Fuyang, China, in 1994, the M.S. degree from Xidian University, Xi'an, China, in 1997, and the Ph.D. degree from Southeast University, Nanjing, China, in 2002. From 2009 to 2010, he held a visiting post-doctoral position with The University of Texas at Dallas. In 2005, he joined the School of Electronic and Optical Engineering, Nanjing University of Science and Technology, Nanjing, where he is currently a Professor and a Supervisor of the Ph.D. and graduate students. He has authored about 200 papers, of which over 80 are in archival journals, including 14 papers in IEEE Journals and 35 SCI-indexed papers. He holds two Chinese patents. His research interests include wireless networks, wireless location, and array signal processing.

BRANKA VUCETIC (M'83–SM'00–F'03) received the B.S.E.E., M.S.E.E., and Ph.D. degrees from The University of Belgrade in 1972, 1978, and 1982, respectively, all in telecommunications. She has held various research and academic positions in Yugoslavia, Australia, U.K., and China. She currently holds the Peter Nicol Russel Chair of Telecommunications Engineering with The University of Sydney and the Director of the Center of Excellence in Telecommunications. She has authored over 300 research papers and co-authored four books in telecommunications and coding theory. Her most significant research contributions have been in the field of channel coding and its applications in wireless communications. Her research has involved collaborations with industry and government organizations in Australia and several other countries.

XIAOHU YOU (F'11) received the B.S., M.S., and Ph.D. degrees from the Nanjing Institute of Technology, Nanjing, China, in 1982, 1985, and 1989, respectively, all in electrical engineering. From 1987 to 1989, he was with the Nanjing Institute of Technology as a Lecturer. Since 1990, he has been with Southeast University as an Associate Professor and a Professor. His research interests include mobile communications, adaptive signal processing, and artificial neural networks with applications to communications and biomedical engineering. He has contributed over 40 IEEE journal papers and two books in the areas of adaptive signal processing, neural networks, and their applications to communication systems. He was the Premier Foundation Investigator of the China National Science Foundation. From 1999 to 2002, he was the Principal Expert of the C3G Project, responsible for organizing China's 3G Mobile Communications Research and Development Activities. From 2001 to 2006, he was the Principal Expert of the National 863 FuTURE Project. He was selected as an IEEE Fellow due to his contributions to development of mobile communications in China in 2011. He received the excellent paper prize from the China Institute of Communications in 1987 and the Elite Outstanding Young Teacher Awards from Southeast University in 1990, 1991, and 1993. He was also a recipient of the 1989 Young Teacher Award of Fok Ying Tung Education Foundation, State Education Commission of China. He is currently the Chairman of the IEEE Nanjing Section.